Gliadin-mediated green preparation of Hybrid Zinc Oxide Nanospheres With Antibacterial Activity and Low Toxicity

Qun Wang
Taizhou University
Peng Ji (jipeng0213@163.com)
Taizhou University
Yansheng Yao
Yangzhou University
Yi Liu
Taizhou University
Yajie Zhang
Taizhou University
Xianglong Wang
Taizhou University
Yuhang Wang
Taizhou University
Jinyan Wu
Fudan University

Research Article

Keywords: zinc oxide, wheat gliadin, bacteriostasis, self-assembly, nanosphere

Posted Date: March 15th, 2021

DOI: https://doi.org/10.21203/rs.3.rs-289730/v1

Abstract

The development of inorganic antibacterial agents that impart antibacterial properties to biomaterials has attracted widely attention. The paper introduced a kind of hybrid nanosphere antibacterial agent composed of wheat gliadin (WG) and zinc oxide (ZnO), with antibacterial effecacy and low toxicity. The ZnO/WG hybrid nanospheres were environment-friendly integrated by molecular self-assembly co-precipitating and freeze-drying transformating, and were characterized using X-ray diffraction (XRD), Fourier Transform infrared spectroscopy (FTIR), Scanning electron microscope (SEM), Atomic absorption spectroscopy (AAS), bacteriostasis test and safety evaluation. It was found that the prepared hybrid nanospheres were composed of two components, ZnO and wheat gliadin, with a diameter scope of 100~200 nm. The content of ZnO in the hybrid nanospheres can reach 46.9~70.2% (w/w); The anti-bacteria tests proved that the prepared ZnO/WG nanospheres (containing 70% ZnO) have an significant inhibitory effect on E. coli (E.C.) and Staphylococcus aureus(S.A.) while the suspension concentration of the nanospheres was above 5 mg/mL. Furthermore, the ZnO/WG nanospheres are relatively safe and highly effective in cells and mice. Therefore, the prepared novel ZnO/WG hybrid nanospheres were supposed to apply in the preparation of anti-infective wound dressings, tissue engineering skin scaffold materials, food and cosmetics preservatives, and so on.

Introduction

Metal-based drugs, especially inorganic nanomaterials used in implantable biomaterials, have been studied as a next-generation nanomedicine[1,2]. However, implanted biomaterials, long or short periods close contacting with human tissue, have the problem of causing various bacterial infections[3-6]. Therefore, the improvement of the antibacterial properties of biomaterials has become the key to their wider application in clinical medicine.

It is one of the methods to improve the antimicrobial properties of biomaterials by inserting antimicrobial substances into biomaterials. Antibacterial substances can be divided into four categories: antibiotics, heavy metals or metal oxides, quaternary ammonium salts, and other cationic surface-active molecules. However, when loaded into biomaterials, the antibiotics will be quickly exhausted, and this approach can easily make bacteria resistant; Besides, although the antibacterial effect of quaternary ammonium salts is better, the application is also limited, due to the hemolytic effect of quaternary ammonium salts[7].

Inorganic antibacterial agents are durable and less toxic[8]. Metal or metal oxide nanoparticles (such as silver, copper, titanium, magnesium, zinc, etc.) are currently the main research directions of inorganic antibacterial agents[9,10]. Nano-ZnO has attracted extensive attention due to its advantages, such as long-term antibacterial, safety, stability, excellent angiogenesis, and promotion of proliferation of adult dermal fibroblast cells[11-13].

Composite nanomaterials obtained by integrating organic and inorganic components have broad application prospects in many fields. Notably, these nanocomposite particles also inherited the superior

characteristics of the raw materials and obtained other multi-functional characteristics that are not available in a single component. For example, a growing number of researchers pay attention to the design of core-shell structured composite nanospheres, which can reduce their toxicity by covering other materials[14-16], and increase their biocompatibility and water dispersibility[17-19].

In this paper, a hybrid nanosphere of inorganic antimicrobial ZnO and wheat gliadin was prepared by self-assembly and freeze-drying. This study is aimed to develop an anti-infective pharmaceutical for surgical trauma therapy and to develop a new tissue-engineered skin with persistent anti-infective properties[20-22].

Results And Discussion

Preparation of ZnO/WG nanospheres

Generally speaking, the most common synthesis methods of ZnO nanoparticles were in the presence of surfactants or precipitating agents being associatied with potential toxic effect against the environment and living orgnisms[3]. Attempting to address this issue, the preparation process of ZnO/WG nanospheres, as illustrated in Figure1 and Figure2, was carried out in an environment-friendly manner, avoiding the extreme reaction conditions, harmful chemicals, and toxic by-products, which would contribute better biocompatibility to the final applications of the nanospheres. The WG molecules here used, rich in amino, carboxyl and hydroxyl groups, are stabilizing agents triggering the self-assemblly co-precipating of hybrid nanoparticles.

Substantially, according to molecular orbital theory, Zn^{2+} have four empty orbitals and are SP^3 hybrids, so Zn^{2+} are easy to form tetra-ligand compounds when there are enough ligands as amine ligand et al. Therefore, the possible formation mechanism of ZnO/WG nanospheres is illustrated as follows:

$$Zn^{2+} + NH_2\text{-R-COOH} \longrightarrow [ZnO(NH_2\text{-R-COOH})_4]^{2+} \quad (1)$$

$$[ZnO(NH_2\text{-R-COOH})_4]^{2+} + 2OH^- \longrightarrow [Zn(OH)_2(NH_2\text{-R-COOH})_2]\downarrow + 2(NH_2\text{-R-COOH}) \quad (2)$$

$$2[Zn(OH)_2(NH_2\text{-R-COOH})_2]\downarrow \xrightarrow{\text{frezze-drying}} 2[ZnO(NH_2\text{-R-COOH})_2]\downarrow + H_2O\uparrow \quad (3)$$

(note: NH_2-R-COOH, representing WG proteins or polypeptides)

The formation process of ZnO/WG nanospheres were shown in above three formulations. Firstly, complexes were self-assembly formed by Zn^{2+} and WG polypeptides; secondly, two hydroxyl groups substituted two NH_2-R-COOH ligands, which resulted in the co-precipitating formation of zinic hydroxic conjugating with WG polypeptides; finally the co-precipitates lost water and transformated to the ZnO/WG nanospheres during the frezze-drying process.

Actually, the transformation between the zinic hydroxic conjugates and ZnO/WG nanospheres, should be confirmed by XRD test and FTIR test, as analyzed below.

XRD analsis

As shown in Figure 3, due to the presence of ZnO crystals in the sample, the XRD pattern of the nano-ZnO has nine characteristic peaks, including: 31.8°, 34.5°, 36.4°, 47.8°, 56.8°, 62.9°, 66.5°, 68.0°, 69.1°. And same peaks also appeared in ZnO/WG nanospheres, including: 31.8°, 34.5°, 36.4°, 47.8°, 56.8°, 62.9°, 66.5°, 68.0°, 69.1°, indicating that ZnO crystals also exist in the ZnO/WG nanospheres, so it was judged that the ZnO/WG nanospheres contained ZnO components in crystalline style[24,25].

Furthermore, in the XRD patterns of ZnO/WG sample, peaks appeared at 31.3°,58.6° , different with the characteristic peaks of ZnO, were possiblly due to the crystallization of WG molecules in the sample.

FTIR analysis

In Figure 4, 3000-3600cm^{-1} is the composite peak formed by the O-H stretching vibration of the -COOH group and the N-H stretching vibration of the -NH_2 group; peaks near 1659 cm^{-1} are the C=O stretching vibration peak of the amide bond, peaks near 1540 cm^{-1} are formed by the N-H stretching vibration of the amide bond, peaks near 1450 cm^{-1} are formed by the C-N stretching of the amide bond; these peaks are typical characteristic peaks of proteins. Furthermore, due to the stretching vibration of Zn-O, peak near 417cm^{-1} appeared the characteristic peak of ZnO. Therefore, according to the comparison among the three FTIR graphs, it was proved that the ZnO/WG nanospheres were composed of ZnO and WG, which is consistent with the XRD analysis results.

Morphorlogy obsevation and anlysis of ZnO/WG nanospheres

The SEM images of ZnO/WG nanospheres were shown in Figure 5. When the WG concentration in the preparation process is 2 mg/mL, 6 mg/mL, 8 mg/mL, 10 mg/mL, the nanospheres are spherical or ellipsoidal, with no holes on the surface, but there is a certain amount of adhesion between the particles; when the WG concentration is 4 mg/mL, the shape of the prepared nanospheres appeared a more irregular spherical shape with rough surface, but the independence between the particles is better. In conclusion, the common profiles of the prepared hybrid nanospheres were revealled: the shape is nearly spherical, the particle size range is 100~200 nm, but the adhesion between the particles is relatively serious. The separation process between the supurnatant and procipatates, as well as the freeze-drying method might has a great influence on the adhesion of ZnO/WG nanospheres, which should be further researched in the following work.

According to the above obsevation of morphology, the particles size changed with the WG concentration increasing. Furthermore, as shown in Figure 6, the ZnO content of the five different samples varied with the concentration of WG used in the preparation process, and its range reached 46.9 ~70.2% (w/w). Especially, when the WG concentration was 4 mg/mL, the average particle size of the correpongding

nanospheres reached a maximum value of 197 nm, and the ZnO content also reached a maximum value of 70.2% (w/w). Therefore, the particles size and the content of the ZnO were functions of the concentration of WG

Analysis of antibacterial test results

As shown in Figure 7, the antibacterial effect of the prepared hybrid nanospheres is represented by a circular sterile area. When the same volume of medicine (25mL per sample) with different concentrations, were dripped onto the agar plate, the inhibitory effect of the nano-particles on microorganisms can be indirectly tested depending on the concentration change of the suspension. The detailed results were given in Table I and discussed as follow.

Table I. Antibacterial Effect of ZnO/WG nanospheres on *E.C.*and *S.A.*

sample	Saline	ZnO nano-power suspension concentration (mg/mL)				The concentration of ZnO/WG hybrid nanosphere suspension (mg/mL)			
		10	5	2	1	10	5	2	1
E.C.	-	++	++	++	-	++	+	-	-
S.A	-	+++	++	+	-	+++	++	-	-
Antibacterial Effect	´	Ö	Ö	Ö	´	Ö	Ö	´	´

(notes:

while D≥10mm, and no bacteria colony in the inhibition zone, recorded as +++;

while D≥10mm, but appeared visible colonies in the inhibition zone, recorded as ++;

while 10mm >D≥5mm, and no colony in the inhibition zone, it is recorded as ++;

while 10mm>D≥5mm, but appeared visible colonies in the circle, it is recorded as +;

while D<5mm, recorded as -.)

Taking ZnO/WG hybrid nanospheres with a ZnO content of 70% (w/w) as an example, it can be found from Table I: Negative control (saline) has no bacteriostatic activity; positive control (ZnO nanopowder), at a concentration of 2mg/mL, has a certain bacteriostatic effect on *E.C.* and *S.A.*; ZnO/WG hybrid nanospheres, at a concentration of 5mg/mL, have a certain bacteriostatic effect on *E.C.* and *S.A.*. At a concentration of 10mg/mL, Both the hybrid nanospheres and the ZnO nanopowder have obvious antibacterial effect on *E.C.* and *S.A.*. This shows that the prepared ZnO/WG hybrid nanospheres have antibacterial activity increasing with the concentration[26,27].

Besides, compared with ZnO nano-powder, at the low concentration, 2mg/mL and 5mg/mL, the bacteriostatic effect of ZnO/WG hybrid nanospheres on *E.C.* reduced; but at the concentration of 10mg/mL, the antibacterial activity on *S.A.* is equivalent. This shows that: Increasing the concentration of ZnO/WG hybrid nanospheres, can produce the equivalent bacteriostatic effect as the ZnO nano-power,

which is beneficial to the application of ZnO/WG hybrid nanospheres, as a candidate antibacterial agents, in the fields of antibacterial biomaterials, food and cosmetics preservatives, etc[28,29].

Analysis of safety evaluation

To further evaluate the potential of ZnO/WG nanospheres in biomedical applications, the biocompatibility of the ZnO/WG nanospheres in vivo was examined in a mouse model. The breakdown of red blood cells collected from the mice was negligible for ZnO/WG nanospheres up to 10 mg/mL(Figure 8). For preparation, no significant weight loss was observed in the mice throughout the trial period(Figure 9), and the retention of ZnO/WG nanospheres in the heart, liver, and kidneys did not cause severe side effects, according to H&E staining(Figure 10), elucidating no serious adverse effects and elucidating good biocompatibility of ZnO/WG nanospheres in vivo[30]. These results generally indicated that the administration of ZnO/WG nanospheres was biocompatible in mice[31].

Conclusion

Generally, ZnO/WG nanospheres were prepared by zinc chloride solution using the selfassembly-freeze drying method, under the induction of WG, at a suitable pH value.

Based on the XRD and FTIR analysis, it was confirmed that the nanosphere was composed of ZnO and WG. Based on the SEM test, it was observed that the shapes of ZnO/WG nanospheres were nearly spherical, with a diameter range of 100 ~ 200 nm. According to AAS data, it was determined that the content of ZnO in the nanospheres reaches 46.9 ~ 70.2% (w/w). The antibacterial test of the bacteriostatic circle method was used and, it was confirmed that the ZnO/WG nanospheres have a good inhibitory effect on *E.C.* and *S.A.*. Moreover, the hemolysis assays and H&E staining demonstrated that ZnO/WG nanospheres had relatively low toxicity in cells and mice.

Methods

Materials

Gluten protein powder (5000Da, food-grade, Jiangsu Zhihui Biotechnology Co., Ltd., China); zinc chloride ($ZnCl_2$), ethanol, sodium hydroxide (NaOH), acetic acid(analytically pure, Sinopharm Group Chemical Reagent Co., Ltd. , China); Zinc (99.99%, premium-grade, Sinopharm Group Chemical Reagent Co., Ltd., China); Concentrated hydrochloric acid(analytical grade, Wuxi City Yasheng Chemical Co., Ltd., China)

Female Balb/c mice (5–6 weeks old) were obtained from the Laboratory Animal Center of China Pharmaceutical University. All animal procedures were performed following the Guidelines for the Care and Use of Laboratory Animals of Taizhou University and approved by the Animal Ethics Committee of Taizhou University.

FTIR-650 Fourier Transform Infrared Spectrometer (FTIR)(FTIR-650, Tianjin Gangdong Technology Co., Ltd., China); Ultima IV X-ray Diffraction Analyzer (XRD)(Ultima IV, Japan Rigaku Co., Ltd., Japan); Sigma-500 Field Emission Scanning Electron Microscope (SEM)(Sigma-500, Carl Zeiss, Germany); SCIENTZ-10N freeze dryer (Ningbo Xinzhi Biotechnology Co., Ltd., China); TAS-990AFG atomic absorption spectrophotometer (AAS)(Beijing Purkinje General Instrument Co., Ltd., China)

Preparation methods

Preparation of wheat gliadin(WG) solution

The process diagram of wheat gliadin (WG) solution is shown in Figure1. About 4g wheat gluten protein powder was slowly poured into 200 mL 70% ethanol solution after stirring for 2h, and centrifuged to obtain supernatant and precipitate; bottom sediment was poured into 200 mL 70% ethanol solution under stirring. In the medium, stirring was continued for another 2h, and the supernatant was centrifuged and combined with the previous supernatant, and concentrated by rotary evaporation to obtain a WG solution with a concentration of 1% (w/w).

Preparation of ZnO/WG nanospheres

The process diagram of ZnO/WG nanospheres is shown in Figure2. Firstly, the above prepared solution of WG, was filled in 5 beakers, each 50.00mL respectively, in which 200.00mL, 75.00mL, 33.50mL, 12.50mL, and 0mL of 60% ethanol were added subsequently, to obtain five kinds of WG solutions with different concentrations of 2mg/mL, 4mg/mL, 6mg/mL, 8mg/mL, 10mg/mL. And then 125.00mL, 62.50mL, 41.75mL, 31.25mL, 25.00mL solutions, each containing 250mg $ZnCl_2$, were respectively added into the five kinds of WG solutions; and subsequently, the pH value of the five WG solutions was adjusted to 8~8.9 using 1 mol/L NaOH aqueous solution. And thus the mixed solutions were rested for 60min, at a 37 ℃ water bath, until the self-assembled particles were completely precipitated. Lastly, the mixed suspension was dialyzed to neutrality in 60% ethanol, using a dialysis membrane (molecular weight cutoff of 12000 Da), in which the retained precipitates were transferred to a Petri dish and freeze-dried at -40 ℃ in a freeze dryer (SCIENTZ-10N, Ningbo Xinzhi Biotechnology Co., Ltd.) for 24h, to obtain the hybrid nanospheres.

Property characterization

The XRD spectrum of the dried nanosphere sample was measured by X-ray diffractometer: line source of Cu targeted Ka, the wavelength of 0.15406nm, scanning step length of 0.03°, scanning range of 10-90°; the infrared spectrum of the sample was measured by FTIR: The dried nanospheres and dried potassium bromide solid powder are mixed, grinded, and compressed to carry out a spectral scan. The scanning wavenumber range was 4000-500 cm^{-1}; after dispersing the prepared dried nanospheres on conductive tape sticked to the aluminum plate, and vacuuming, SEM was used to observe and take photos; AAS was used to determine the Zn element content in the sample, and then calculate the ZnO content (3 parallel

samples); a particle size analysis software of Nano Measurer was used to measure the average particle size of the nanospheres (number of samples 40), based on the SEM photos.

Evaluation of Antimicrobial Activity

Firstly the prepared ZnO/WG hybrid nanosphere sample (containing a ZnO mass ratio of 70.2%) and the positive control sample (commercially available nano-ZnO) were subjected to ultraviolet irradiation sterilization. Then, In the ultra-clean workbench with the cleanliness of class B, the dry particles of hybrid nanospheres were prepared into physiological saline suspensions of 10 mg/mL, 5 mg/mL, 2 mg/mL, 1 mg/mL, 0 mg/mL (respectivelly marked as a, b, c, d, e). After the activated E.C. and S.A. (approximately 10^8 Cfu/mL) were evenly coated on the agar solid medium (TSA) and standed still for 5 minutes until the bacterial suspension was absorbed by the agar plate, 25μL each of the above four different concentrations of nanosphere suspensions, as well as negative control sample, were dropped into the TSA medium previously coated with bacteria. After about 10 minutes later until the nanaparticle suspensions were absorbed by the agar plate, the cultures were inverted in a 32°C microbial incubator and incubated for 24h, finally to observe whether there is an inhibition zone at the drop sites, record the diameter (D) of the appeared inhibition zone.

Safety evaluation

Hemolysis

1 mL of the whole blood of the mice was taken and put into a 2 mL centrifuge tube containing 2.5 μL of 2% heparin sodium and stirred slowly. Afterward, the same volume of saline solution was added and centrifuged at 1500rpm for 10min. The supernatant was removed and resuspended with 10mL saline. The suspension was centrifuged at 1500rpm for 20min. The same process was repeated three times to obtain red blood cells[23]. Subsequently, 0.2 mL erythrocyte suspension was mixed with (I) 0.8 mL PBS as a negative control, (II) 0.8 mL deionized water as a positive control, and (III) 0.8 mL aqueous dispersion of ZnO/WG nanospheres (1-10 mg/mL). After incubation at 37◦C for 1 h and centrifuged at 12000rpm for 5min, the supernatants were taken to determine the optical density (OD value) in a microplate reader (Spark 10 M, Tecan, Zürich, Switzerland) at a wavelength of 540 nm. The calculation formula of hemolysis ratio (Hr) is as follows: Hr (%) =(ODs-ODn/ODp- ODn)×100%, in which ODs, ODp, and ODn are the OD values of the samples, the positive control, and the negative control, respectively.

Histological studies

To further evaluate the potential of ZnO/WG nanospheres in biomedical applications, we evaluated the possible biosafety and adverse reactions for 10 days. Female Balb/c mice were randomly divided into 2 groups (n = 3), and Intragastric administration (1) 0.9wt% saline, (2) ZnO/WG nanospheres (10 mg/kg) every days. The body weight as an index of systemic toxicity was recorded and calculated every two days. After 10 days of treatment, major organs (including heart, liver, and kidney) were cut, half-sectioned,

photographed, and then placed in a buffered 4% formaldehyde solution overnight. Deparaffinized 5 μm sections were stained with hematoxylin-eosin for further analysis.

Statistical Analysis

Use SPSS Statistics 17.0 software to check all data and express them as mean±standard deviation (SD). Use Student's *t*-test to analyze statistical significance; *p <0.05 was considered the minimum meaning.

Declarations

Acknowledgements

This work was supported by the Key Program of Taizhou University (TZXY2014ZDKT010); Scientific Research Starting Foundation of Taizhou University (TZXY2020QDJJ009); Science and Technology Innovation Action Plan of Shanghai Science and Technology Commission□19441909900)

Author contributions statement

Q. Wang and P. Ji conceived the experiments , discussed the results and wrote the main manuscript text. Q. Wang prepared the figures1-7 and Table 1, Ji prepared figures8-10, Y. Yao , Y. Liu, Y. Zhang, X. Wang and Y. Wang conducted the experiments, J. Wu analysed the results. All authors reviewed the manuscript.

Competing interests

The authors have no competing interests as defined by Nature Research, or other interests that might be perceived to influence the results and/or discussion reported in this paper.

References

[1] Jin S.E. & Jin H.E., Synthesis, characterization, and three-dimensional structure generation of zinc oxide-based nanomedicine for biomedical applications. Pharmaceutics **11**, 575, DOI: https://doi.org/10.3390/ pharmaceutics 11110575(2019).

[2] Das S., Mitra S., Khurana S.M.P. & Debnath N. Nanomaterials for biomedical applications. Front Life Sci. **7**, 90-98, DOI: https://doi.org/ 10.1002/biot.202000574(2013).

[3] Cruz D.M., Mostafavi E., Vernet-Crua A., Barabadi H., Shah V., Cholua-Díaz J. L, Guisbiers G. & Webster T. J. Green nanotechnology-based zinc oxide (ZnO) nanomaterials for biomedical applications: a review, J. Phys. Mater. **3**, 034005, DOI: https://doi.org/10.1088/2515-7639/ab8186(2020).

[4] Campoccia D., Montanaro L. & Arciola C.R. A review of the clinical implications of anti-infective biomaterials and infection-resistant surfaces. Biomaterials **34**, 8018-8029, DOI: https://doi.org/10.1016/j.biomaterials. 2013.07.048(2013)

[5] Corduas F., Mancuso E. & Lamprou D. A. Long-acting implantable devices for the prevention and personalised treatment of infectious, inflammatory and chronic diseases, J Drug Deliv. Sci. Tec. **60**, 101952, DOI: https://doi.org/ 10.1016/j.jddst.2020.101952(2020).

[6] Kuijer R., Jansen E. J P, Emans P. J, Bulstra S., Riesle J., Pieper J., Grainger D. W. & Busscher H. J. Assessing infection risk in implanted tissue-engineered devices. Biomaterials **28**, 5148-5154, DOI: https://doi.org/10.1016/ j.biomaterials.2007.06.003(2007).

[7] Song W. & Ge S. Application of antimicrobial nanoparticles in dentistry. Molecules **24**,1033, DOI: https:// doi.org/ 10.3390/molecules24061033(2019).

[8] Chen R., Han Z., Huang Z., Karkl J., Wang C., Zhu B. & Zhang X. Antibacterial activity, cytotoxicity and mechanical behavior of nano-enhanced denture base resin with different kinds of inorganic antibacterial agents, Dent. Mater. J. **36**, 693-699, DOI: https:// doi.org/. 10.4012/dmj.2016-301(2017).

[9] Bradley E.L., Castle L. & Chaudhry Q. Applications of nanomaterials in food packaging with a consideration of opportunities for developing countries. Trends Food Sci. Tech. **22**, 604-610, DOI: https:// doi.org/ 10.1016/j.tifs.2011.01.002(2011).

[10] Chaudhry Q., Scotter M., Blackburn J., Ross B., Boxall A., Castle L., Aitken R. J. & Watkins R. Applications and implications of nanotechnologies for the food sector. Food Addit. Contam. A **25**, 241-258, DOI: https:// doi.org/ 10.1080/02652030701744538(2008).

[11] Carofiglio M., Barui S., Cauda V. & Laurenti M. Doped Zinc Oxide Nanoparticles: Synthesis, Characterization and Potential Use in Nanomedicine. Appl. Sci **10**, 5194, DOI: https:// doi.org/ 10.3390/app10155194(2020).

[12] Ahtzaz S., Nasir M., Shahzadi L., Amir W., Anjum A., Arshad R., Iqbal F., Chaudhry A. A., Yar M.& Rehman I. A study on the effect of zinc oxide and zinc peroxide nanoparticles to enhance angiogenesis-pro-angiogenic grafts for tissue regeneration applications. Mater. Design **132**, 409-418, DOI: https://doi.org/10.1016/ j.matdes.2017.07.023(2017).

[13] Cui L., Liang J., Liu H., Zhang K. & Li J. Nanomaterials for Angiogenesis in Skin Tissue Engineering. Tissue Eng. Part B Re. **26**,203-216, DOI: https:// doi.org/ 10.1089/ten.TEB.2019.0337(2020).

[14] Song Q., Peng M., Wang L., He D. & Ouyang J. A fluorescent aptasensor for amplified label-free detection of adenosine triphosphate based on core-shell Ag@SiO2 nanoparticles. Biosens. Bioelectron. **77**, 237-241, DOI: https:// doi.org/10.1016/j.bios.2015.09.008(2016).

[15] Kim M., Son H., Kim G. , Park K. & Huh Y. Redoxable heteronanocrystals functioning magnetic relaxation switch for activatable T1 and T2 dual-mode magnetic resonance imaging. Biomaterials **101**, 121-130, DOI: https:// doi.org/ 10.1016/j.biomaterials.2016.05.054(2016).

[16] Iribarnegaray V., Navarro N., Robino L., Zunino P., Morales J. O. & Scavone P. Magnesium-doped zinc oxide nanoparticles alter biofilm formation of Proteus mirabilis. Nanomedicine-UK **14**, 1551-1564, DOI: https:// doi.org/ 10.2217/nnm-2018-0420(2019).

[17] Wang H., Shen J., Cao G., Gai Z., Hong K., Debata P. R., Banerjee P. & Zhou S. Multifunctional PEG encapsulated Fe_3O_4@silver hybrid nanoparticles: Antibacterial activity, cell imaging and combined photothermo/ chemo-therapy. J. Mater. Chem. B **1**,6225-6234, DOI: https://doi.org/10.1039/ C3TB21055C(2013).

[18] Ji P., Huang H., Yuan S., Wang L. , Wang S. , Chen Y., Feng N., Veroniaina H. , Wu Z. , Wu Z. & Qi X. ROS-mediated apoptosis and anticancer effect achieved by artesunate and auxiliary Fe(II) released from ferriferous oxide-containing recombinant apoferritin. Adv. healthc. mater. **8**, 1900911, DOI: https://doi.org/10.1002/ adhm.201900911(2019).

[19] Ji P., Wang L., Chen Y., Wang S. , Wu Z. & Qi X. Hyaluronic acid hydrophilic surface rehabilitating curcumin nanocrystals for targeted breast cancer treatment with prolonged biodistribution. Biomater. Sci.-UK **8**, 462-472, DOI: https:// doi.org/ 10.1039/C9BM01605H(2020).

[20] Wang J., Wu H., Yang Y., Yan R., Zhao Y., Wang Y., Chen A., Shao S., Jiang P. & Li Y. Bacterial species-identifiable magnetic nanosystems for early sepsis diagnosis and extracorporeal photodynamic blood disinfection. Nanoscale **10**, 132-141, DOI: https:// doi.org/10.1039/C7NR06373C (2018).

[21] Ferrone E., Araneo R., Notargiacomo A., Pea M. & Rinaldi A. ZnO Nanostructures and Electrospun ZnO-Polymeric Hybrid Nanomaterials in Biomedical, Health, and Sustainability Applications. Nanomaterials-Basel **9**, 1449, DOI: https:// doi.org/ 10.3390/nano9101449(2019).

[22] Jatoi A. W., Kim I. S. & Ogasawara H. Characterizations and application of CA/ZnO/AgNP composite nanofibers for sustained antibacterial properties. Mater. Sci. Eng. C **105**, 110077, DOI: https://doi.org/10.1016/ j.msec.2019.110077 (2019).

[23] Du C., Zhou M. X., Jia F., Ruan L., Lu H., Zhang J., Zhu B., Liu X., Chen J., Chai Z. & Hu Y. D-arginine-loaded metal-organic frameworks nanoparticles sensitize osteosarcoma to radiotherapy. Biomaterials **269**, 120642 DOI: https:// doi.org/10.1016/j.biomaterials.2020.120642(2021),.

[24] Dwivedi L. M., Baranwal K., Gupta S., Mishra M., Sundaram S. & Singh V. Antibacterial nanostructures derived from oxidized sodium alginate-ZnO. Int. J. Biol. macromol. **149**, 1323-1330, DOI: https://doi.org/10.1016/ j.ijbiomac.2020.02.011(2020).

[25] Ohira T., Yamamoto O., Iida Y. & Nakagawa Z. Antibacterial activity of ZnO powder with crystallographic orientation. J. Mater. Sci. -Mater M. **19**, 1407-1412, DOI: https://doi.org/10.1007/ s10856-007-3246-8(2008).

[26] Silva B. L., Caetano B. L., Chiari-Andréo B. G., Pietro R. & Chiavacci L. A. Increased antibacterial activity of ZnO nanoparticles: Influence of size and surface modification. Colloid Surfaces B **177**, 440-447, DOI: https:// doi.org/ 10.1016/j.colsurfb.2019.02.013(2019).

[27] Prasanna V. L. & Vijayaraghavan R. Chemical manipulation of oxygen vacancy and antibacterial activity in ZnO. Mater. Sci. Eng. C **77**, 1027-1034, DOI: https:// doi.org/10.1016/j.msec.2017.03.280(2017).

[28] Li Y., Yang Y., Qing Y., li R., Tang X., Guo D. & Qin Y. Enhancing ZnO-NP Antibacterial and Osteogenesis Properties in Orthopedic Applications: A Review. Int. J. Nanomed **15**, 6247-6262, DOI: https://doi.org/10.2147/ IJN.S262876(2020).

[29] Shi L., Li Z., Zheng W., Zhao Y., Jin Y. & Tang Z. Synthesis, antibacterial activity, antibacterial mechanism and food applications of ZnO nanoparticles: a review. Food Addit. Contam. A **31**, 173-186, DOI: https:// doi.org/ 10.1080/19440049.2013.865147(2014).

[30] Xu X., Chen Y., Zhang Y., Yao Y. & Ji P. Highly stable and biocompatible hyaluronic acid-rehabilitated nanoscale MOF-Fe(2+) induced ferroptosis in breast cancer cells, J. Mater. chem. B **8**, 9129-9138, DOI: https:// doi.org/ 10.1039/D0TB01616K(2020).

[31] Bitonto V., Alberti D., Ruiu R., Aime S., Crich S. G. & Cutrin J. C. L-ferritin: a theranostic agent of natural origin for MRI visualization and treatment of breast cancer. J. Control. Release. 319, 300-310, DOI: https:// doi.org/ 10.1016/j.jconrel.2019.12.051(2020).

Figures

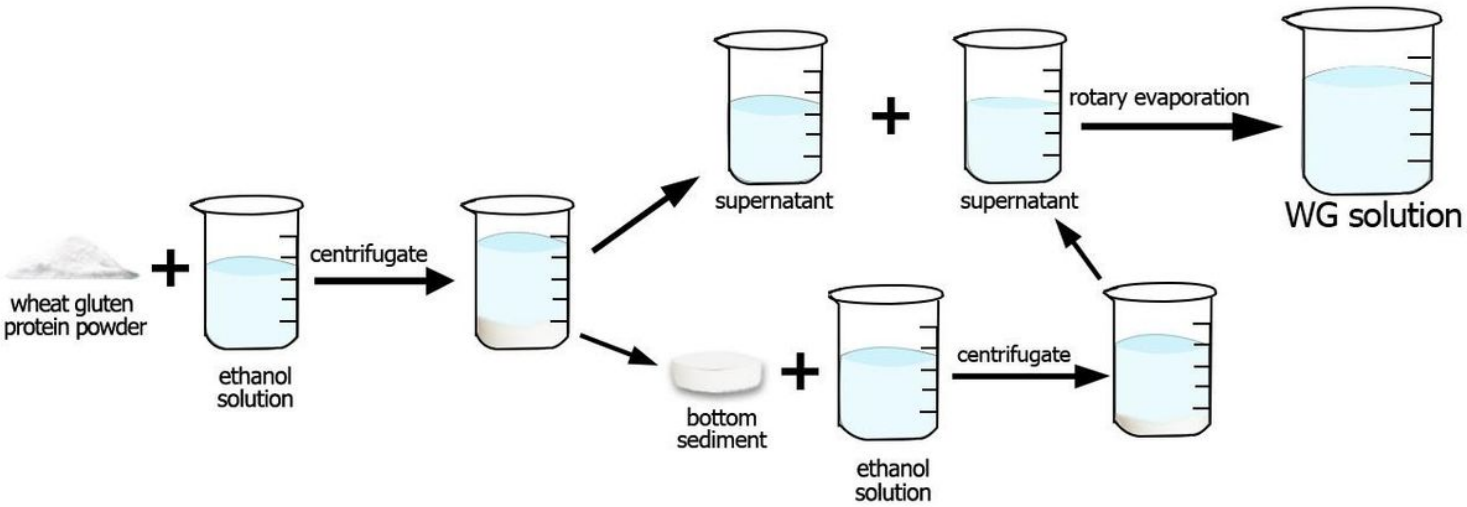

Figure 1

Process diagram of wheat gliadin(WG) solution

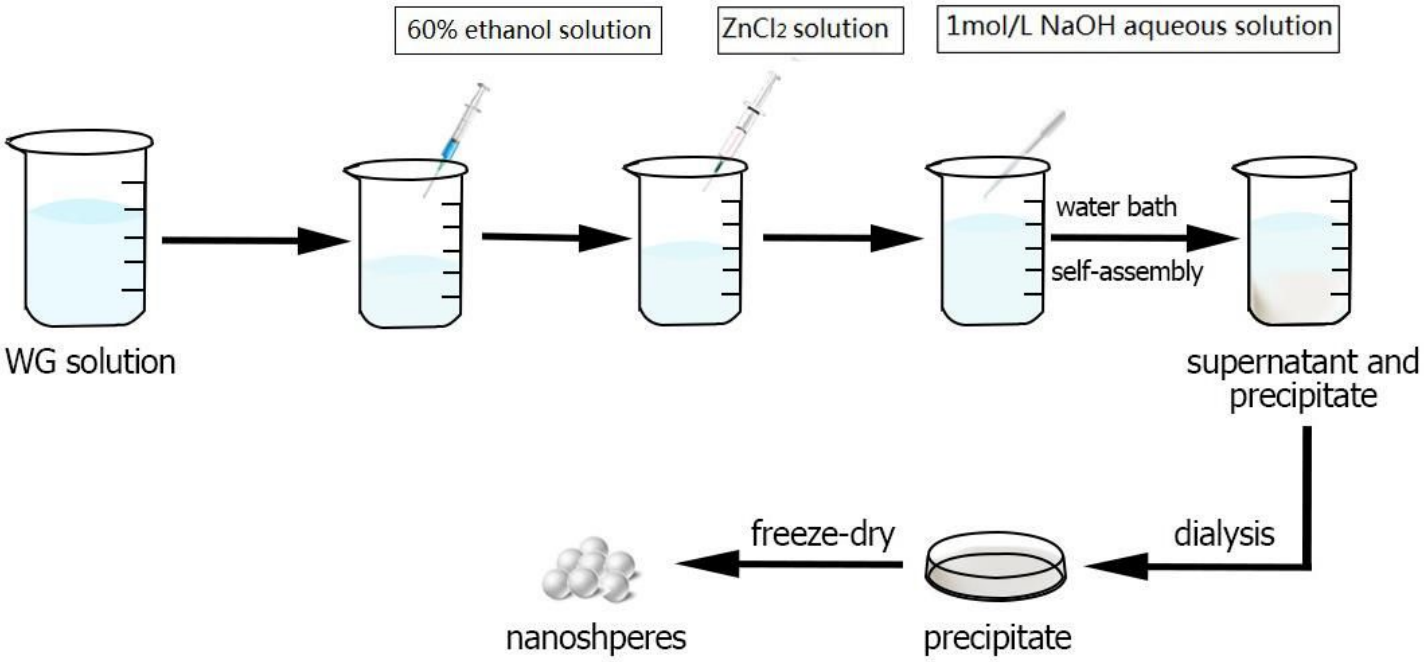

Figure 2

Process diagram of ZnO/WG nanospheres

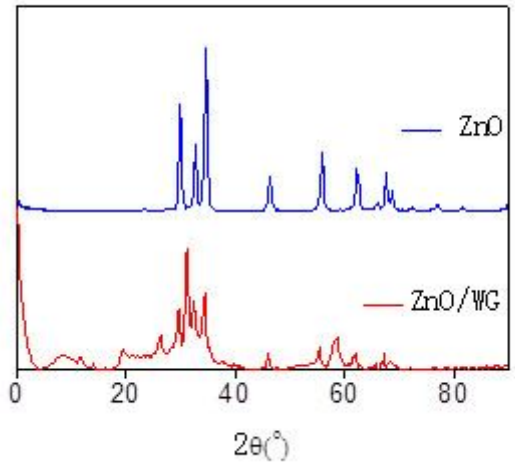

Figure 3

XRD patterns of ZnO and ZnO/WG nano-particles

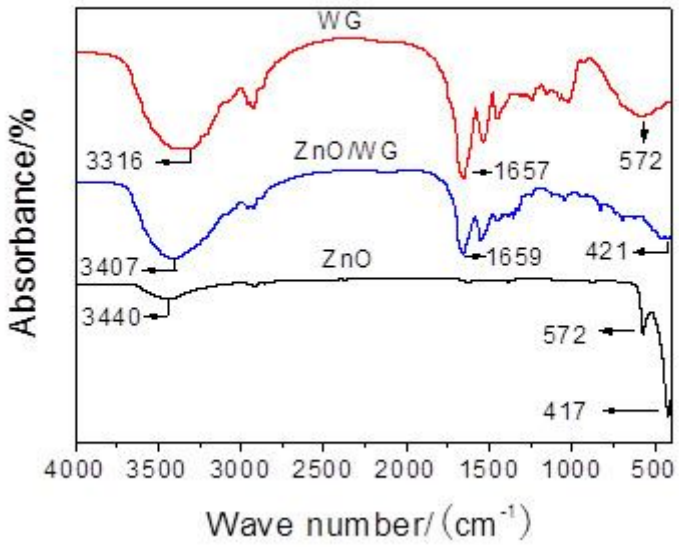

Figure 4

FTIR graphs of nano-ZnO, WG powder and ZnO/WG nanospheres

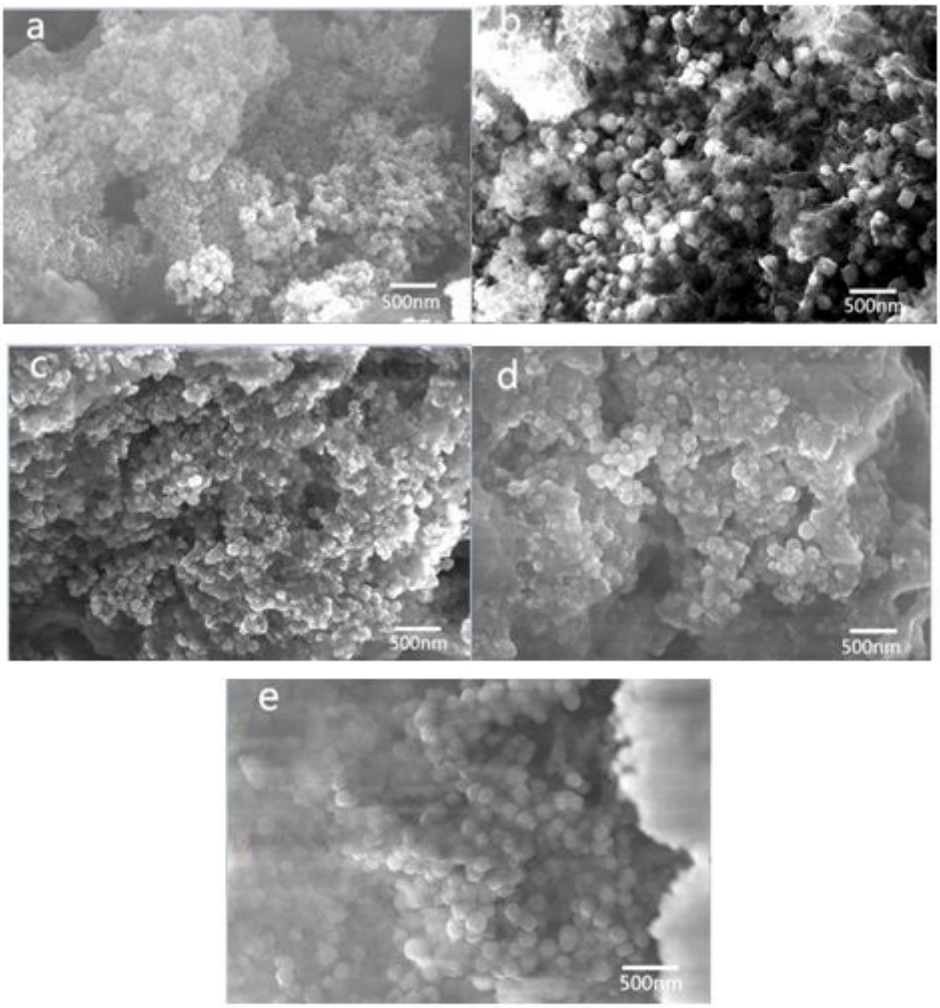

a—2mg/mL； b—4mg/mL； c—6mg/mL； d—8mg/mL； e—10mg/mL

Figure 5

ZnO/WG nanospheres prepared by different concentrations of WG

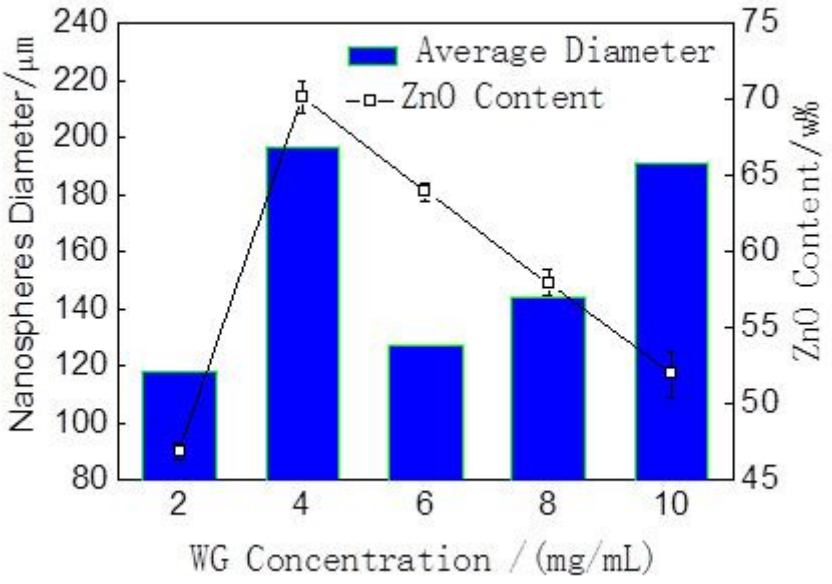

Figure 6

Effect of WG concentrations on the diameter and ZnO content of nanospheres

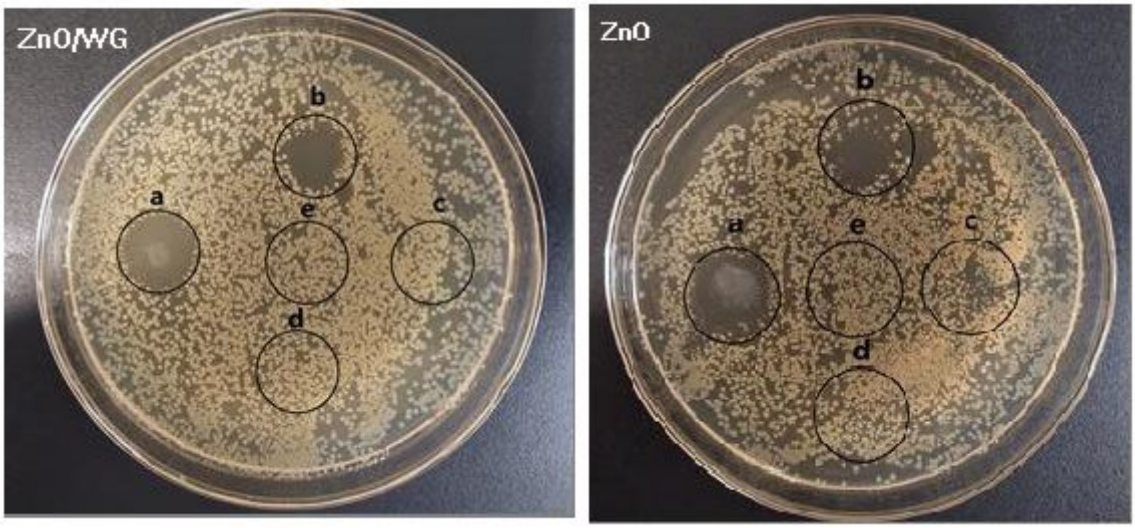

Figure 7

Suspension concentration: a-10 mg/mL,b-5 mg/mL,c-2 mg/mL,d-1 mg/mL,e- saline (notes: left-ZnO/WG nanosphere, right-ZnO nano-power). Represenative sample agar plates showing the zones of inhibition to S.A.

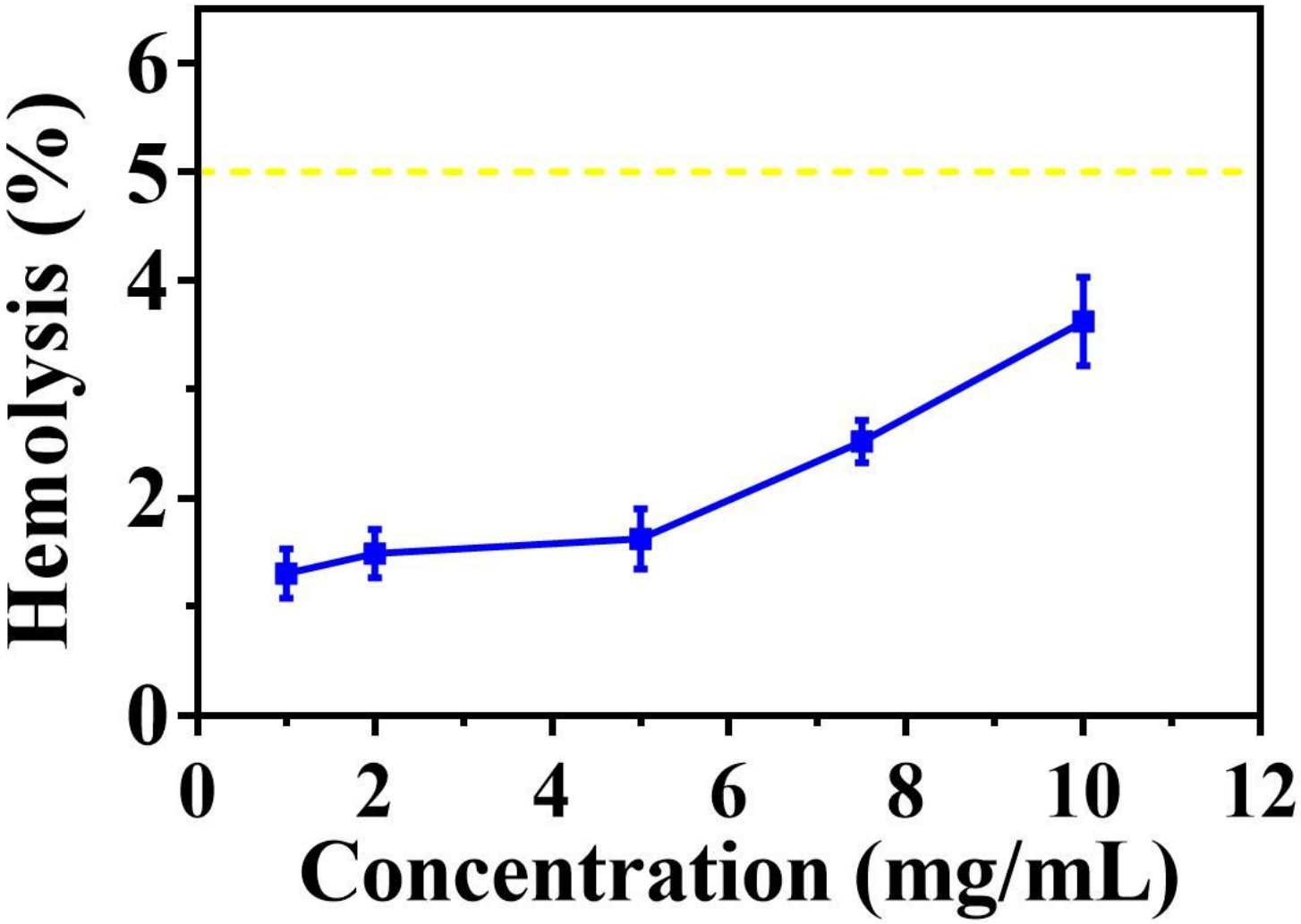

Figure 8

Hemolysis testing results of ZnO/WG nanospheres at various concentrations

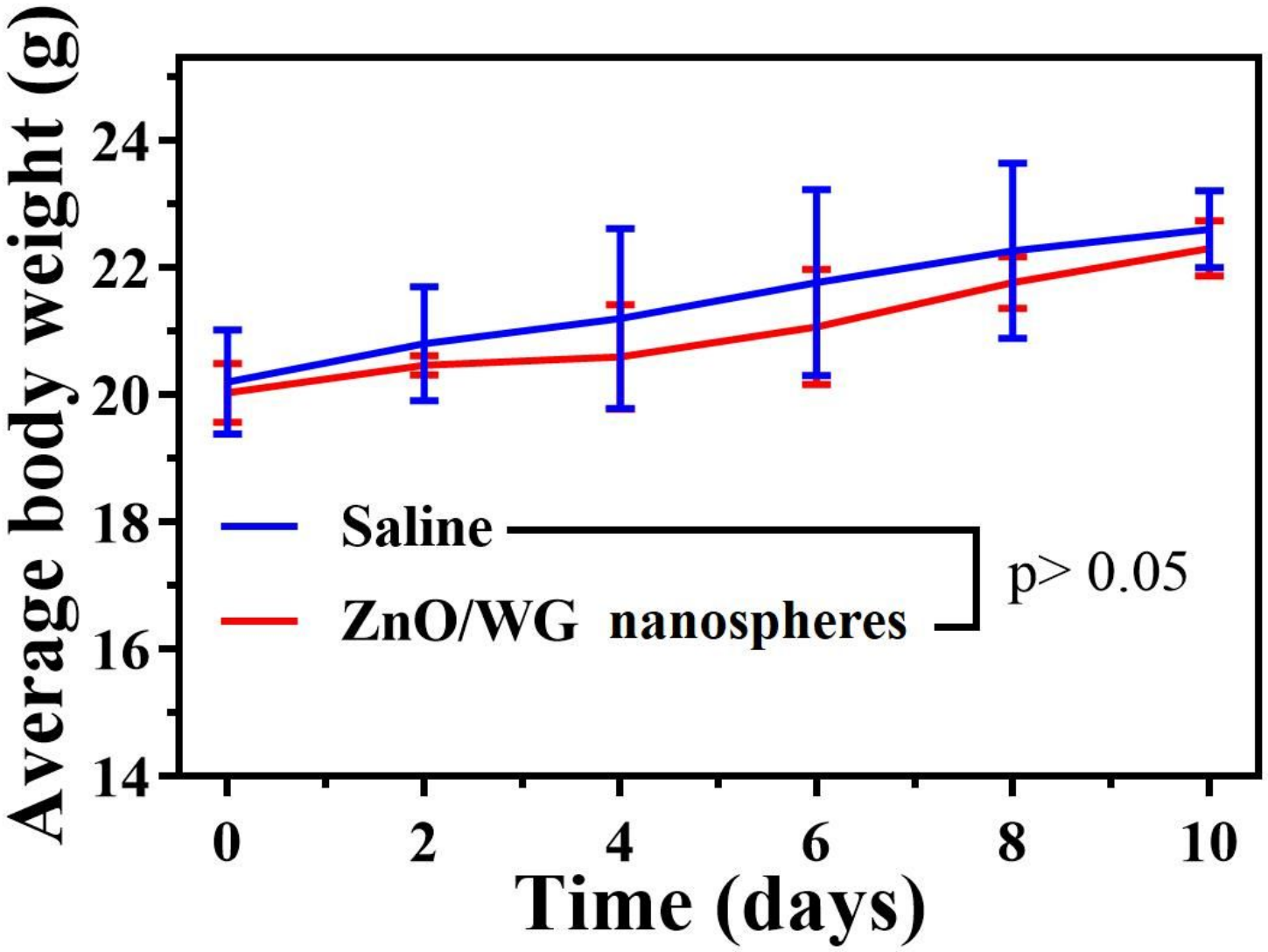

Figure 9

Average bodyweights of ZnO/WG nanospheres during 10-day(n= 3)

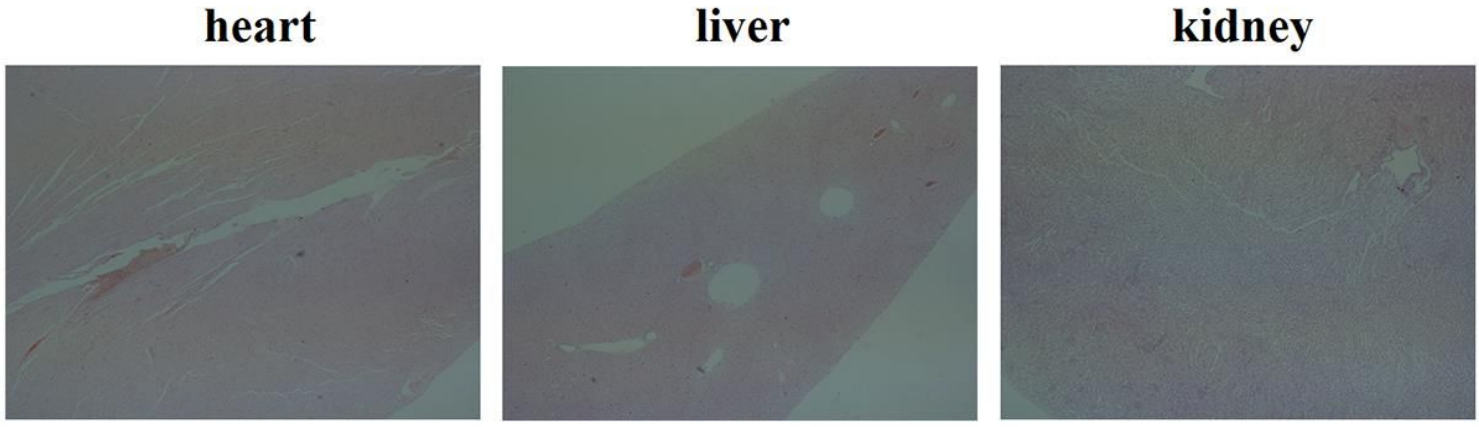

Figure 10

Histological images of the major organs (heart, liver, kidney) were obtained over 10 days after various treatments.